



Techno-Economics Assessment of Geothermal Binary Cycle Power Plant Located in Isolated Grid

Suardi Nur^{* 1}, M. Faisi Ikhwali^{*}, and Nur Aida^{*}

www.ericjournal.ait.ac.th

ARTICLE INFO

Article history:

Received 17 February 2022

Received in revised form 17

May 2022

Accepted 07 June 2022

Keywords:

Binary cycle power plant

EES simulation

Geothermal energy

Techno-economic assessment

Thermodynamic modeling

ABSTRACT

Jaboi geothermal project experiences a long delay since its concession winning bidder declared in 2008. Based on the latest study, Jaboi geothermal resource can produce up to 40 MW electricity. However, resource location in an isolated grid island that has limited electricity demand is the constraint for its development. In the current study, we propose a conceptual design of a geothermal power plant adapted the load profile in an isolated electricity grid such as in Sabang City, Weh Island, in Indonesia. The electricity generated in the island is not able to be transmitted to the main island of Sumatra. Therefore, to be viable the power plant must be designed to follow the demand existed on the island. To design a demand-based power plant, we perform a thermodynamic analysis of a geothermal binary cycle by using Engineering Equation Solver (EES) software. The optimal flow rate of geothermal fluid required to meet the demand is determined. The simulation results reveal that to produce a 3 MW net power output geothermal binary power plant, it requires a total of 95 kg/s geothermal fluid mass flow rate. Theoretically, this mass flow rate can be supplied from one production well. Therefore, a well-doublet system consisting of a production and re-injection wells can be deployed as the most economic option.

1. INTRODUCTION

Indonesia is estimated to own 28,910 MWe of geothermal resources [1]. Fauzi [2] classifies a total of 7,886 MWe as low temperatures resources and 16,134 MWe resources with temperatures over 190°C. However, these resources have not been employed optimally with only 7.3% or 2,108.5 MW of Indonesia's geothermal resources utilized to generate electricity by 2019 as shown in Table 1.

Based on geological, geophysical, hydrological, and engineering criteria, a geothermal system can be categorized as volcanic, sedimentary, geopressed and hot dry rock or enhanced geothermal system (EGS) [3]. Meanwhile, Hochstein and Browne [4] classify geothermal system according to its nature of heat transfer systems as hydrothermal, volcanic and volcanic-hydrothermal systems. Hydrothermal system is a system where the heat transfer from a heat source to the surface done by convection involving meteoric fluid with or without trace of magmatic fluids. In contrast to that, in volcanic system the heat is transferred to the surface by convection that involves magmatic fluid from magmatic chambers. The volcanic-hydrothermal combines systems where the ascending magmatic fluid mixed with meteoric fluid. The reservoir temperature of these system is classified as:

1. High enthalpy (the reservoir temperature is over 225°C)
2. Medium enthalpy (the reservoir temperature between 125 and 225°C)
3. Low enthalpy (the reservoir temperature is lower than 125°C)

The development of small-scale geothermal resource of low to medium enthalpy system is quite challenging due to the selection of technology and relatively low financial viability. In the case of Jaboi geothermal resource, aside from those issues, the location of resources in isolated grid become an extra constraint on the resource's utilization.

1.1 The Resources of Jaboi Geothermal

Jaboi geothermal working area is sited at Suka Jaya district under the administration of city of Sabang in the Weh Island, Indonesia. Initially, the Weh Island was a quaternary age volcano part of western Indonesia volcanic arc.

Jaboi geothermal prospect reconnaissance was started in 1972 with the purpose to observe the surface manifestations and continued with geo-electrical surveys between 1983 and 1984. More detailed geological survey was done in 2000. The surveys involve geo-chemical and geophysical surveys such as geo-magnetic, resistivity, gravity, and geo-electrical were completed between 2005 and 2006 [5].

Jaboi geothermal resource is assumed as a water dominated geothermal system with the top layer of reservoir is estimated at the depth of 600 to 800 m [6]. The central reservoir is estimated to be 1000 m deep.

^{*}Department of Environmental Engineering, Universitas Islam Negeri Ar-Raniry Banda Aceh, Banda Aceh, Indonesia.

¹ Corresponding author:

Email: suardinur.fst@ar-raniry.ac.id

Based on Landsat-8 image analysis, the surface temperature ranges between 22 and 29°C [7]. This information is essential in calculating the temperature at 1000 m depth in Section 3.1.

The stratigraphy of Weh Island consists of four main geological formations. The rock formation of Weh Island composed of tertiary sedimentary which is the oldest layer, tertiary-quadernary, quadernary volcanic, limestone and quadernary alluvial rocks [6].

More detailed lithology of Weh Island is explained in [8], [9]. The tertiary sedimentary rock is composed of tuffaceous sandstone which is estimated to be from Miocene age (Tms). The outcrop of this rock can be found on the eastern coast of Weh Island. The younger lithology of tertiary-quadernary volcanic rocks consists of lava flow unit (QTvw) and pyroclastic flow unit (QTapw).

Table 1. Existing Geothermal Power Plants in Indonesia by 2020.

No	Field	Province	Developer/Project owner	MW
1	Sibayak	North Sumatra	Pertamina Geothermal Energy (PGE)	12
2	Ulubelu	Lampung	PGE	220
3	Salak Mt.	West Java	Star Energy	377
4	Wayang Windu	West Java	Star Energy	227
5	Kamojang	West Java	PGE	235
6	Darajat	West Java	Star Energy	270
7	Dieng	Central Java	Geodipa Dieng Energy	60
8	Lahendong-Tompaso	North Sulawesi	PGE	120
9	Ulumbu	East Nusa Tenggara	PT. PLN (Persero)	10
10	Mataloko	East Nusa Tenggara	PT. PLN (Persero)	2.5
11	Patuha	West Java	Geodipa Dieng Energy	55
12	Sarulla	North Sumatra	Sarulla Operation Limited	330
13	Karaha	West Java	PGE	30
14	Lumut Balai	South Sumatra	Pertamina Geothermal Energy (PGE)	55
15	Sokoria	East Nusa Tenggara	PT. Sokoria Geothermal Indonesia	5
16	Sorik Merapi	North Sumatra	PT. Sorik Merapi Geothermal Power	45
17	Muara Laboh	West Sumatra	PT. Supreme Energy Muara Laboh	85
Total				2,108.5

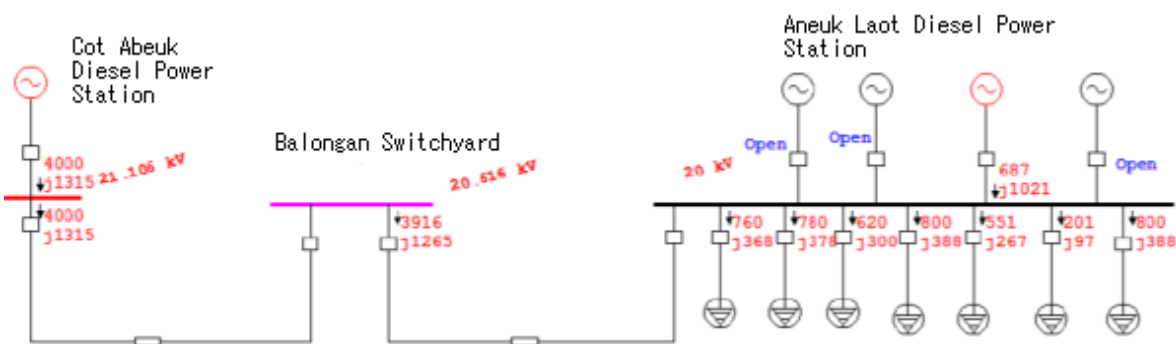


Fig. 1. Power flow configuration of 20 kV electricity grid system in city of Sabang. Source: Septian [10]

1.2 Electricity Demand in Sabang

As of now the electricity demand in Sabang is supplied from diesel fuelled power plants with peak load around 5 MW. Figure 1 shows the power flow of 20 kV electricity grid system in Sabang. It can be seen the

power system has two diesel power stations consisting of 5 units of diesel generators with a total installed capacity of 8 MW, however only two units of 4 MW and 1 MW are operated to serve the loads.

Geothermal power plants are a baseload-type power plant. Therefore, to design a demand-based

optimized power plant that is intended to serve a base load type, it is important to estimate the baseload of the electricity systems. The annual baseload can be estimated by using Equation 1:

$$\text{Baseload} = \text{Peak load} \times \text{Load Factor} \quad (1)$$

The baseload estimation based on the peak load data and load factor growths is plotted in Figure 2. It can be seen that the baseload of thw electricity grid in Sabang by 2020 is around 3.2 MW.

Meanwhile, the electricity consumption is increased moderately with an estimation approximately 30 GWh by 2021. The electricity grid in Sabang is an isolated grid system, therefore the electricity produced in the island is unable to be transmitted to another load area. The electricity demand per sector in Sabang is presented in Figure 3. It pertains that the public sector has the highest growth rate about 7.3 %, followed by household and commercial sectors that share the same growth rate of 6.6%. Meanwhile, the industrial sector has the lowest growth rate of 1.7%.

Peak load and Base load Electricity System in Sabang

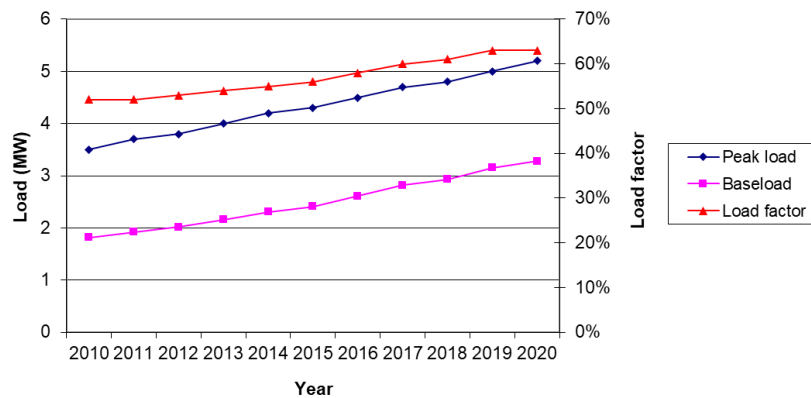


Fig. 2. The estimated baseload growth of the electricity grid in Sabang.

Projection Electricity Demand Per Sector

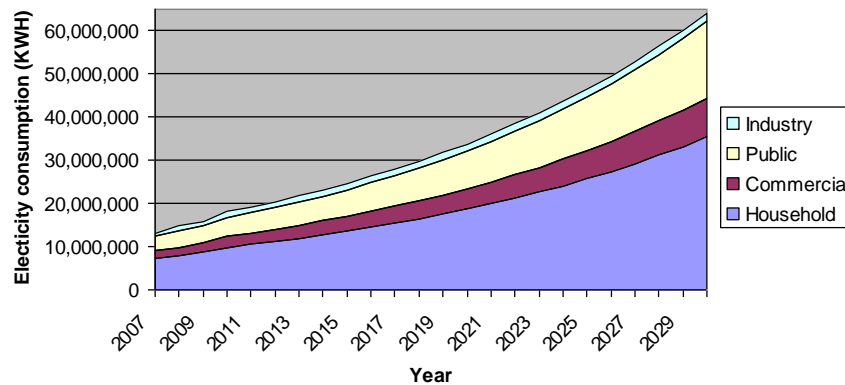


Fig. 3. Projection of electricity demand growth in Sabang by 2030.

2. THERMODYNAMICS OF GEOTHERMAL BINARY CYCLE POWER PLANT

In Indonesia, the single flash system of geothermal power plants is found as the most common type of geothermal power plant employed [11]. Meanwhile, the binary cycle type of power plants are commonly deployed for medium or low temperature geothermal systems such as enhanced geothermal system (EGS) [12].

The binary cycle power plant uses a secondary fluid to convert the heat into power. In this context, the heat from geothermal fluid is transferred to a secondary

working fluid, normally an organic working fluid through heat exchangers. The secondary working fluid circulates in a closed cycle system. At specific boiling-point, the working fluid evaporates, expands through a turbine and releases enthalpy [13].

Organic Rankine Cycle (ORC) and Kalina Cycle are the most common types of binary cycle used for geothermal power plants. ORC is a simplified Rankine cycle with organic materials employed as the working fluids, while in the Kalina type of binary cycle, the mixture of ammonia and water is typically employed as the secondary working fluid. The mixture compositions

are not constant at all states of the cycle. Basically, Kalina cycle is a Rankine cycle equipped with extra distillation and absorption units.

2.1 The Thermodynamic Cycles

A comprehensive thermodynamic cycle analysis that involves pumps, turbine, condenser as well as the cooling system is essential in designing a geothermal binary cycle power plant. The analysis is performed based on fundamental thermodynamic principles as given by first law of thermodynamics. As shown in

Figure 4, key parameters that determine technical specifications of a geothermal binary cycle power plant include temperature and mass flow rate of geothermal fluid, the pressure of the well-head, reinjection, and ambient temperatures. Geothermal fluid mass flow rate and temperature are specific according to the natural characteristic of reservoirs. However, the reinjection temperature is defined through careful analysis by considering the brine saturation index to avoid the scaling of precipitates such as silica in the pipes and heat exchangers [14].

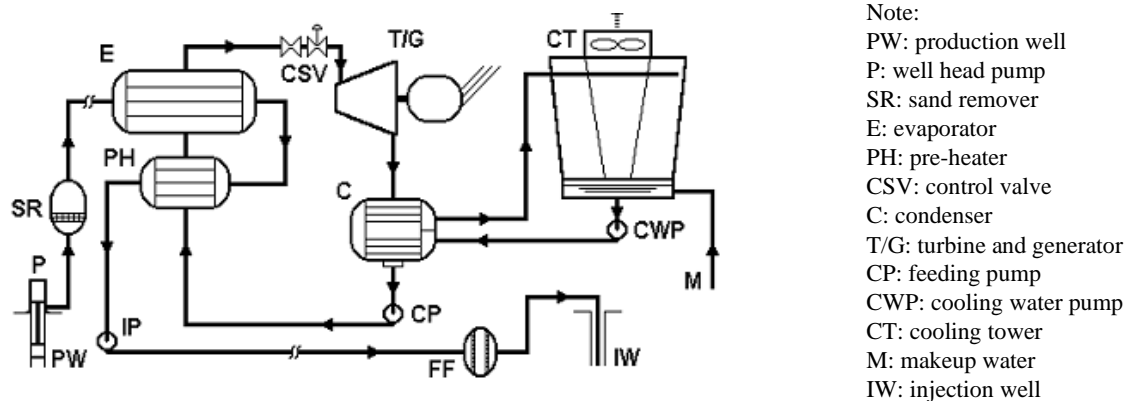


Fig. 4. Flow diagram of typical binary geothermal power plant [13].

Turbine Analysis

As high-pressure vapor of an organic working fluid expands in the turbine, part of the internal energy of pressurized working fluid is converted as kinetic energy by the turbine. The power output of the turbine is given by Equation 2 [13]:

$$\dot{W} = \dot{m}_{wf}(h_1 - h_2) = \dot{m}_{wf}\eta_t(h_1 - h_{2s}) \quad (2)$$

Where,

- η_t refers to the efficiency of isentropic turbine
- h_{2s} refers to the state of exhaust from ideal isentropic turbine
- \dot{m}_{wf} is mass flow rate of working fluid.
- h_1 and h_2 refer to the enthalpy in the inlet and outlet of the turbine.

Condenser Analysis

The exhaust steam from the turbine is condensed in a condenser. Condenser performance is one of the parameters that determine the efficiency of a binary power plant. In condenser, the heat from the working fluid is rejected to the cooling mediums *i.e.* water or air. The amount of heat rejected to cooling medium is given by Equation 3:

$$\dot{Q} = \dot{m}_{wf}(h_2 - h_4) \quad (3)$$

Where,

- \dot{m}_{wf} refers to the mass flow rate of working fluid
- $(h_2 - h_4)$ refers to the enthalpy of working fluid at the inlet and outlet of the condenser

The relationship of the working fluid mass flow rate and the cooling water mass flow rate is given by Equation 4:

$$\dot{m}_{cw}(h_y - h_x) = \dot{m}_{wf}(h_2 - h_4) \quad (4)$$

or

$$\dot{m}_{cw}\bar{c}(T_y - T_x) = \dot{m}_{wf}(h_2 - h_4) \quad (5)$$

Where,

- \bar{c} is the heat capacity of cooling water
- T_y and T_x refer to the temperature difference at the inlet and outlet of the condenser.

In this simulation, T_x is desired temperature of isopentane to be cooled down in this case 320 K or 46°C. T_y is the temperature of isopentane when entering the condenser (temperature outlet of turbine indicated as T_2 in the model flow diagram as depicted in Figure 6).

Feed Pump Analysis

Power consumption of feed pumps to pressurize the working fluid is given by Equation 6:

$$\dot{W}_p = \dot{m}_{wf}(h_5 - h_4) = \dot{m}_{wf}(h_{5s} - h_4)/\eta_p \quad (6)$$

where

- η_p refers to isentropic pump efficiency
- h_{5s} refers ideal isentropic pump.

Heat Exchanger Analysis

Two heat exchangers are employed in the cycles as preheater and evaporator. The energy balance of these heat exchangers is analysed separately. It is assumed

that the heat exchangers are properly insulated, thus all the heat from geothermal fluid is transferred to working fluid or there is no heat loss in heat exchangers [15], [16]. Furthermore, the mass flow rate is assumed constant, therefore the differences of the potential energy and kinetic energy entering and leaving the heat exchangers are negligible. The relationship between geothermal mass flow rate and working fluid mass flow rate is given in Equations 7:

$$\dot{m}_b(h_a - h_c) = \dot{m}_{wf}(h_1 - h_5) \quad (7)$$

According to DiPippo [13], in the case of geothermal fluid having low dissolved gases and solids, Equation 7 may be rewritten as in Equation 8:

$$\dot{m}_b \bar{c}_b (T_a - T_c) = \dot{m}_{wf} (h_1 - h_5) \quad (8)$$

Where,

- T_a is temperature of brine at the inlet
- T_c is brine injection temperature
- C_b is average specific heat of brine

Cooling System Analysis

Geothermal power plants are typically cooled by using air, water with a cooling tower or direct water as cooling mediums. In this study, we use the force draught air-cooled cooling system. The energy balance between hot water and cold air in the cooling tower can be seen in Figure 5:

The parameters in Figure 5 are described below:

For the water:

- W_a : Mass of hot water entering the cooling tower (kg/s)
- H_{fa} : Enthalpy of water entering the cooling tower (kJ/kg)
- W_b : Mass of cold water exiting the cooling tower (kg/s)
- H_{fb} : Enthalpy of water exiting the cooling tower (kJ/kg)

For the air:

- m_{air} : mass flow rate of air (kg/s)
- h_{a1} : cold dry air enthalpy (kJ/kg)
- ω_1 : cold air humidity ratio
- h_{g1} : cold-water vapor enthalpy (kJ/kg)
- h_{a2} : hot dry air enthalpy (kJ/kg)
- ω_2 : hot air humidity ratio
- h_{g2} : hot water vapor enthalpy (kJ/kg)

The dry air flows through the cooling tower remains unchanged. As the circulating water subsequently loses mass due to evaporation, while in contrast the water vapor in the air gains mass from the evaporated water, based on a unit mass of dry air (m_a), therefore the required make-up cooling water can be calculated as in Equation 9:

$$W_a - W_b = \dot{m}_a \cdot (\omega_2 - \omega_1) \quad (9)$$

Where $W_a - W_b$ is the make-up water mass flow rate (W_{mw}). The energy balance in the cooling tower can be rewritten as in Equation 10.

$$\begin{aligned} \dot{m}_{air} \cdot h_{g2} + W_a h_{fa} \\ = \dot{m}_{air} \cdot h_{g1} + W_a h_{fb} \\ + W_{mw} h_{fa} \end{aligned} \quad (10)$$

$$\begin{aligned} \dot{m}_{air} \cdot (h_{g2} - h_{g1}) - \dot{m}_{air} \cdot (\omega_2 - \omega_1) \cdot h_{fa} \\ = W_a (h_{fb} - h_{fa}) \end{aligned} \quad (11)$$

$$\dot{m}_{air} = \frac{W_a (h_{fb} - h_{fa})}{(h_{g2} - h_{g1}) - (\omega_2 - \omega_1) \cdot h_{fa}} \quad (12)$$

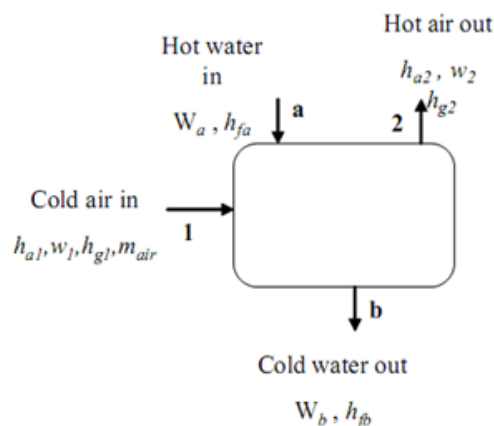


Fig. 5. Energy balance in the cooling tower [17].

2.2 Auxiliary Power Demand

In a binary cycle, the auxiliary power means the power demand required to supply the fluid loop consisting of a downhole pump ($P_{aux,TW}$), a feed pump ($P_{aux,bin}$) and cooling systems ($P_{aux,cool}$). To calculate the auxiliary power for the geothermal fluid loop, Equation 13 is used [18]:

$$P_{auxTW} = \dot{V}_{TW} (-\rho_{TW} g h_{DFL}) + \Delta p_{fr} + p_{wh} + \frac{1}{\eta_{dp}} \quad (13)$$

where h_{DFL} , ρ_{TW} , g , Δp_{fr} , p_{wh} and η_{dp} are notations used to refer respectively the dynamic fluid level, geothermal fluid volume flow rate, geothermal fluid density, gravity

constant, friction losses in production well, wellhead pressure and downhole pump efficiency.

The auxiliary power for the feed pump in binary unit ($P_{aux,bin}$) depends on the flow rate and density of working fluid ρ_{wf} . Thus, its auxiliary power demand can be calculated by Equation 14:

$$P_{aux,bin} = \frac{\dot{m}_{wf}}{\rho_{wf}} (p_v - p_c) \frac{1}{\eta_{FP}} \quad (14)$$

Notation of $P_{aux,bin}$, ρ_{wf} , p_v , p_c , η_{FP} and \dot{m}_{wf} respectively refer to auxiliary power demand for working fluid feeding pump, the density of working fluid, working fluid evaporation and condensation pressures, feed pump efficiency and working fluid mass flow rate.

The auxiliary demand for a wet cooling tower and fans to generate the forced draught is calculated by Equation 15:

$$P_{aux,cool} = P_{aux,CP} + P_{aux,fans} \quad (15)$$

where $P_{aux,CP}$ and $P_{aux,fans}$ are the power demand for cooling water pump and fans respectively. While the auxiliary demand for water cooling pump can be calculated as in Equation 16:

$$P_{aux,CP} = \frac{\dot{m}_{cw}}{\rho_{cw}} (\Delta P_{cw} + \rho_{cw} g h_{fill}) \frac{1}{\eta_{CP}} \quad (16)$$

where, ρ_{cw} , ΔP_{cw} , h_{fill} , and η_{cp} are respectively refer to cooling water mass flow rate, density of cooling water, friction losses, the height of cooling tower fill and cooling pump efficiency. The auxiliary power required for the fans is calculated by using the equation:

$$P_{aux,fan} = \frac{\dot{m}_a}{\rho_a} \Delta p_{fan} \frac{1}{\eta_{fan}} \quad (17)$$

where, \dot{m}_a and ρ_a are the mass flow rate of air and density of air, respectively.

3. ASSUMPTION USED IN THE SIMULATIONS

The purpose of this conceptual design is to propose a model of a binary cycle power plant that able to produce 3 MW net power output. The authors used Engineering Equation Solver (EES) software to perform the simulation. EES software are helpful in providing solutions to solve complex algebraic equations including solving differential equations, complex variable equations, and parameter optimization of a thermodynamic model. EES software can simultaneously identify and group the equations. Additionally, EES provides numerous built-in mathematical and thermophysical properties that is helpful in solving engineering calculations. The steam tables of thermodynamic properties are available as a built-in feature that includes organic working fluids, methane, ammonia, carbon dioxide and other fluid properties commonly used as secondary working fluids.

The simulation purpose in this study is to determine the brine mass flow rate required to produce a 3 MW net power output. Key parameters used in the model is specified in Table 2.

The simulated parameters and results are presented in Table 3 and meanwhile the conceptual design based on these results is shown as in Figure 6.

Table 2. Key parameters applied in the model.

Input parameters	Notation	Designed value
Brine temperature	T_{brine}	200°C
Evaporator pressure	P_e	1700 kPa
Temperature of inch-point	T_{pp}	5°C
Well head pressure	$P_{wellhead}$	18 bar
Cooling Water Temperature	$T_{cw in}$	25°C
wet bulb temperature	T_{wb}	25°C

Table 3. Key simulation output.

Key simulation outputs	Notation	Results
Brine mass flow rate	m	95 kg/s
Working fluid mass flow rate	$m_{isopentene}$	104.6 kg/s
Cooling water mass flow rate	m_{cw}	791.4 kg/s
Make-up cooling water mass flow rate	m_{makeup}	17.35 kg/s
Temperature of reinjected brine	$T_{brine out}$	80.68°C
Gross power produced	P_{gross}	4645 kW
Net power output	P_{net}	3129 kW
Feed-pump power demand	$P_{wf feed pump}$	213.9 kW
Cooling water pump power demand	$P_{cooling water pump}$	73.07 kW
Fans power demand	P_{fan}	223.9 kW
Downhole feed pump power demand	$P_{downhole pump}$	1003 kW

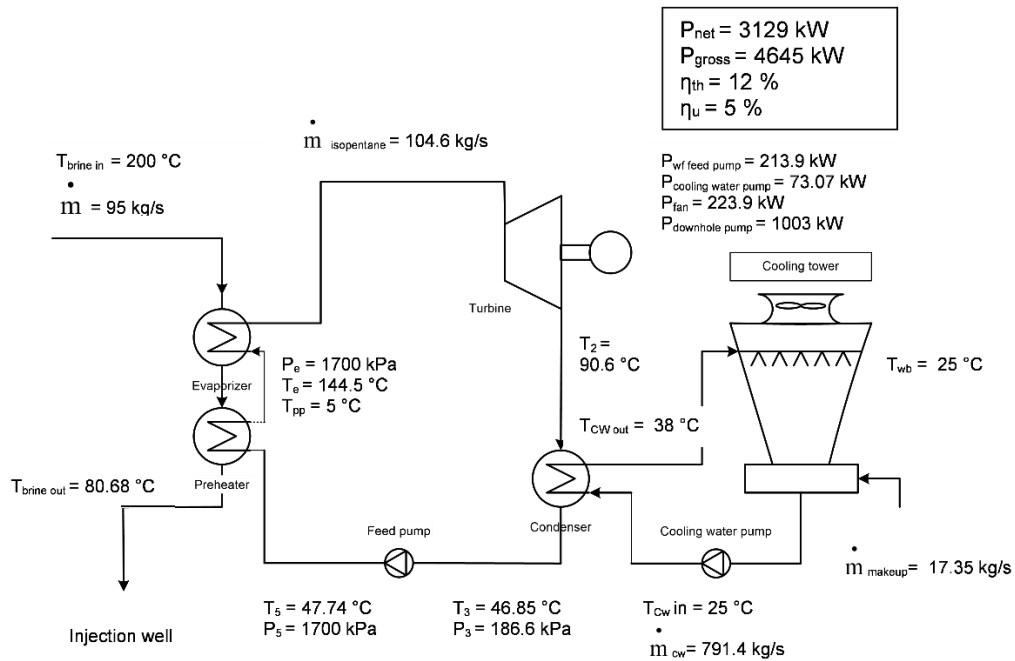


Fig. 6. Conceptual design of Jaboi geothermal binary cycle power plant.

The thermodynamic cycle for ORC power plants is distinguished into subcritical and supercritical. In this study, we design a subcritical geothermal binary cycle power plant with isopentane (i-C₅H₁₂) as secondary working fluid. The evaporation pressure of working fluid in a subcritical cycle, is constantly under the critical pressure. The working fluid absorbs the heat transferred from preheater and evaporator. As the evaporation is at a constant temperature, therefore significant temperature differences occur between the brine-cooling and the working-fluid-heating curve [19].

The selection of secondary working fluids is not only determined by their thermodynamic properties, other specific characteristics such as the stability of temperature, corrosivity, flammability, ozone depletion factor and global warming potential also can be a

consideration. In this simulation, isopentane (C₅H₁₂) is employed as a working fluid. Isopentane with critical temperature of 187.8°C and boiling point at 28°C fits the characteristic of Jaboi geothermal fluid that has estimated temperature of 200°C [16].

3.1 Brine Temperature Estimation

Jaboi geothermal model is revealed in Figure 7. The thermal gradient drilling targets are in the valley between Mt. Seumerugah and Mt. Leumo Matee. Two wells of JBO-1 and JBO-2 have been drilled in 2006 with the purpose to obtain thermal gradient at 250 m depth. The JBO-2 well is successfully drilled to the targeted depth, meanwhile the JBO-1 failed to reach the targeted depth.

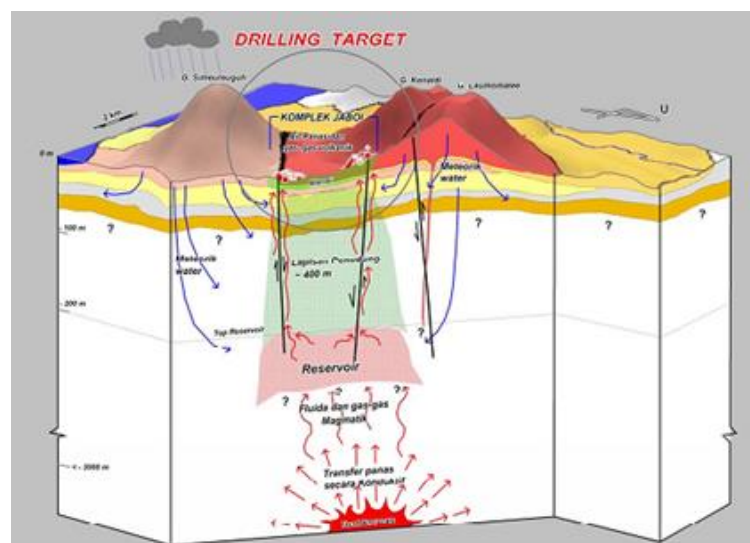


Fig. 7. Jaboi geothermal model [20].

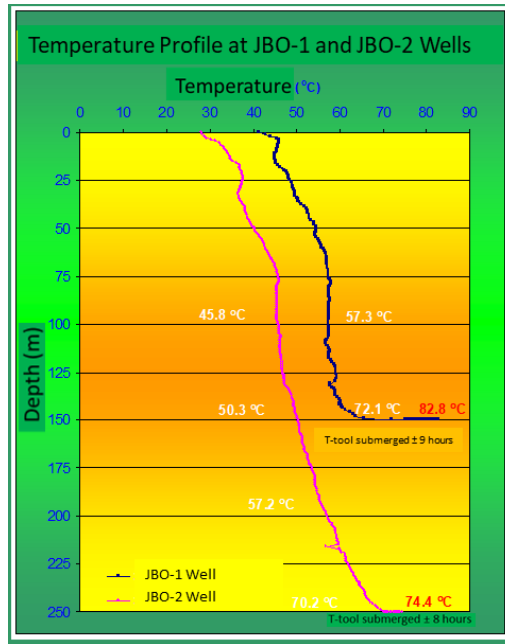


Fig. 8. Thermal gradient profile of Jaboi geothermal drilling JBO-1 and JBO-2 at 250 m and 150 m depth respectively [20].

The temperature read by the probe are 72.1°C and 70.2°C, respectively. However, after the probes are heated-up for few hours (8 and 9 hours), the temperatures rise to 82.8°C and 74.4°C, respectively.

Therefore, based on these thermal gradient drillings, a temperature of 74.4°C is assumed to be the temperature at 250 m depth. As suggested by Munandar *et al.*, (2006), the center of the reservoir of Jaboi geothermal is estimated at the depth of 800 to 1000 m. The temperature at 1000 depth is assumed following Equation 18:

$$Geothermal\ Gradient = \frac{BHT - MAST \times 100}{D} \quad (18)$$

Where:

- BHT refers to the temperature of bottom hole (74.4°C)
- MAST refers to yearly average surface temperature is assumed around 25°C [4].
- D is the depth of the bottom hole in meter. The geothermal gradient is presented in °C/100 m.

Thus, it is calculated that the temperature at the depth of 1000 m is around 200°C.

3.2 Estimation of Well Head Pressure

Well head pressure is closely associated with the geothermal fluid mass flow rate extracted from the wells. Well head pressure selection is influenced by the characteristic of a reservoir, particularly its natural pressure. The well head pressure is assumed to be 18 bars (or 1800 kPa). At this pressure, it is assumed geothermal fluid is not flashed when in the surface plant equipment.

3.3 Other Assumptions used in the Simulation

Other assumptions used in the simulation are listed below:

1. Efficiencies:

- Efficiency of isentropic turbine = 0.75
 - Efficiency of feed pump = 0.8
 - Efficiency of downhole pump = 0.75
 - Efficiency of cooling pump = 0.8
 - Efficiency of generator = 0.95
 - Efficiency of cooling fans = 0.8
2. Pinch-point or minimum difference of heat exchanger temperature (ΔT_{pp}) = 5 °C
 3. Cooling tower
 - The rise of pressure on fans = 170 Pa
 - The height of cooling tower r = 1.5 m
 - Cooling water approach to the wet bulb temperature 3°C
 - The rise of cooling water temperature in the condenser = 13°C
 - Pressure losses = 1 bar
 - The rise of air pressure in the fan in the cooling tower = 170 Pa
 4. Down hole pump [21]
 - Production index (PI) = 160 m³/(h.MPa)
 - Level of static fluid (h_{SFL}) = 295 m
 - Level of dynamic fluid (h_{DFL}) = 597 m
 - Friction loss = 10 kPa
 - Hole casing diameter: 8.5 inch

4. SIMULATION RESULTS

4.1 Evaporation Pressure

The working fluid vapor is assumed saturated at pressure of 1700 kPa, where at this pressure level, the simulation results indicate the optimum net power output as revealed in Figure 9. Net power output decreases when the pressure over 1700 kPa is applied, assumed due to the rise in auxiliary power demand needed for the working fluid feed pump as shown in Figure 10.

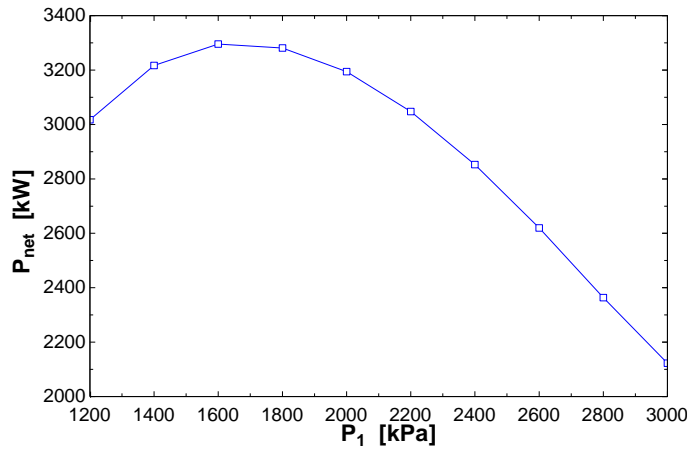


Fig. 9. Optimization of working fluid evaporation pressure.

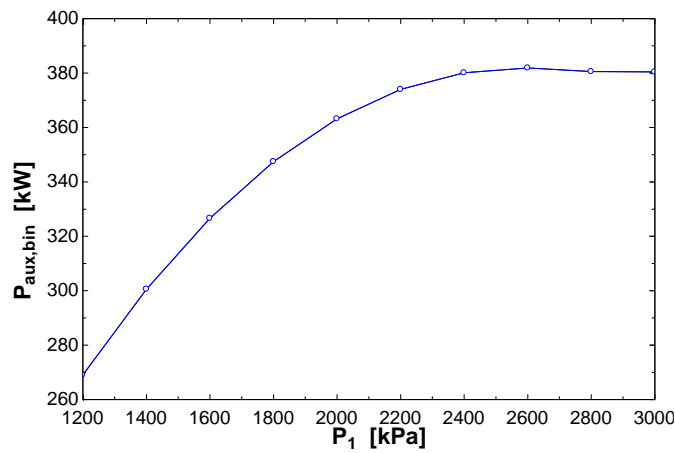


Fig. 10. Power consumed by auxiliary equipment increases in line with the rise of evaporation pressure of the working fluid.

4.2 Brine Mass Flow Rate

The correlation between mass flow rate and power production is plotted in Figure 11. To design a 4.6 MW gross power output, the simulation results show it requires a 95 kg/s geothermal fluid mass flow rate.

4.3 Reinjection Temperature

The simulation shows that the heat from geothermal fluid with a mass flow rate 95 kg/s and temperature of 200°C will raise the isopentane enthalpy to 174.7 KJ/kg.

Preheater is contributed to 56 % of heat transfer to the isopentane as shown in Figure 12. It also can be seen the geothermal fluid is reinjected back to the ground at temperature of 80.68°C. The change of temperatures and entropy at every point is visualized in T-s diagram as depicted in Figure 13. Practically, the reinjection temperature of the geothermal fluid is set to the temperature level of no or minimal scaling problem that occurred in the injection pipeline.

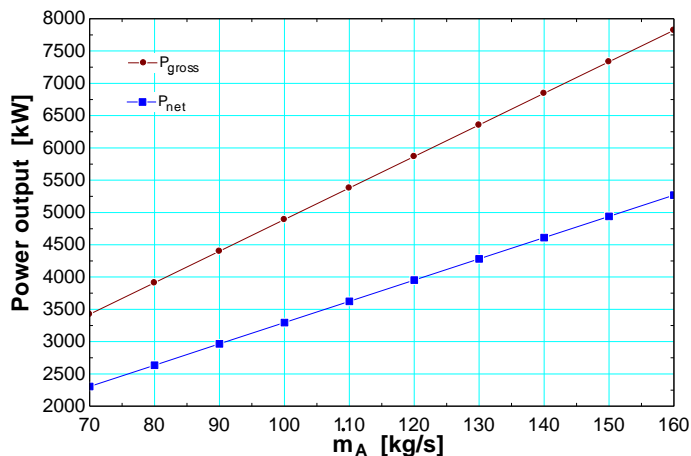


Fig. 11. Optimization of geothermal fluid mass flow rate.

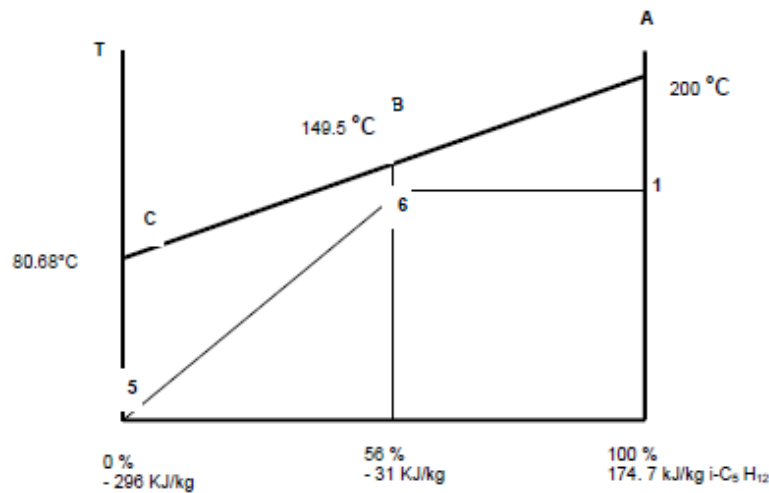


Fig. 12. Temperature – heat transfer diagram.

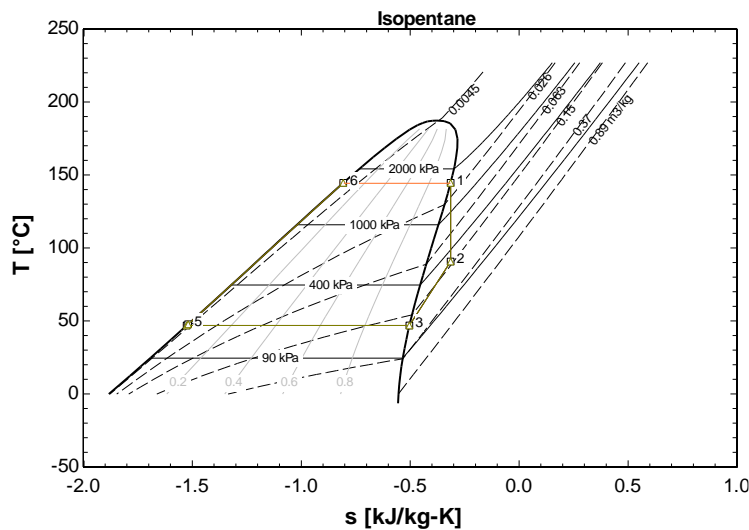


Fig. 13. T-s plot of the designed binary cycle power plant.

4.4 Condensing System

The optimum condensation temperature is highly influenced by ambient temperatures[18]. In this simulation, the exhaust temperature of working fluid steam from the turbine outlet is 90.6°C. The steam goes through the condenser and then the steam is condensed by cold water with a temperature of 25°C which makes the steam temperature drops to 46.85°C. After completing the cooling process, the rejection heat to the cooling water is estimated as 411.6 KJ/kg which raises the cooling water temperature to 38°C.

4.5 Cooling System

The temperature of cooling water from condenser is cooled again in a cooling tower. In this simulation, the forced draft type air cooling tower is used. The mass flow rate of cooling water required is 791.4 kg/s. To pump this water, it needs 73.7 kW of power to pump. The power demand for cooling water pumps is typically between 5 and 20 kW_{el} per MW_{th} of power plant output [18], [22]. The cooling water will experience the losses, consequently the make-up water is required. In this

simulation, it requires 17.35 kg/s mass flow rate of make-up water. The power needed to pump the make-up water is calculated 2.17 kW. The percentage of make-up water required around 1 to 5 % of cooling water mass flow [22].

The cooling process of hot water entering the cooling tower is done by transferring the heat to the cold air with temperature assumed to be equal to dry air temperature (T_{db}) of 25°C or close to the wet bulb temperature (T_{wb}) given the approximated air relative humidity is 100%. After the cooling process, the outlet temperature of the air in the cooling tower will raise to 35°C. Furthermore, to force 1533 kg/s of air, a 223.9 kW auxiliary power demand for fans is required. Typically, in a cooling system, the power demand for fans is between 5 and 10 kW_{el} per MW_{th} [22].

4.6 Auxiliary Power Demand

The total auxiliary power demand required was calculated as 1516 kW or 32 % of gross power output. Therefore, the net power output is 3129 kW. The details of auxiliary power demand required are presented in Table 4.

Table 4. Power demand consumed by auxiliaries.

Auxiliary power demand	Capacity (kW)
Downhole pump	1003
Working fluid feed pump	213.9
Cooling water pump	73.7
Make up water pump	2.17
Cooling tower fans	223.9
Total	1516
Gross power	4645

5. ECONOMIC ASSESSMENT

5.1 Investment Cost

The investment cost for small geothermal project depends significantly on power plant cost, drilling cost, resource quality and cost of financing. The cost is distributed into several activities such as the cost to purchase the surface equipment and the cost for subsurface related activities that include the cost for exploration, steam field development, subsurface drillings and power plant constructions [23].

To optimize the economic value, a 5 MW geothermal binary cycle power plan with a well-doublet system is planned. The system requires only a production well and a reinjection well. Deployment of this type of system is expected to reduce the cost for drillings significantly. In the case of a typical geothermal power plant, the drilling cost is usually to be in the range between 20 and 50% of the total project costs depending on site characteristics and inherent uncertainty [23]. Further drilling to maintain the steam production of a make-up well can be drilled in 4 or 5 years of operation depending on the decline rate of the geothermal reservoir.

Budisulistyo and Krumdieck [24] reported the typical investment cost for binary cycle power plants is between 2500 USD/kW and 5000 USD/kW [19]. The amount can rise if the cost for exploration and drilling is included [19]. We estimate the total investment cost required to develop the Jaboi geothermal binary power plant is US\$ 35 million including the cost for exploration and drilling and other activities as detailed below:

- Geology and geosciences: 1 year
- Exploration and appraisal: 2 years
- Field development: 2 years
- Power plant construction: 1 year

5.1.1 Surface geosciences costs

At this stage, the surface activities that include geological, geochemical, and geophysics surveys are conducted. The aim of these activities is to develop a preliminary conceptual model of geothermal reservoir. The expenditures for geological and geosciences activities are estimated to be US\$ 2.55 million. The exploration cost depends on the countries and the resource specifics [25]. Stefánsson [23] estimates the surface exploration cost is between US\$ 762 and 1192 per kW. Worldwide, the cost required for surface exploration is between US\$ 0.6 and 2 million per MW

[25].

5.1.2 Exploration and appraisal cost

The main activities at this stage are to drill exploration wells, in this case by using slim hole drillings. The advance geological, geochemical, and geophysical surveys to determine the best location for production wells, power plant as well as the access road to the location is also undertaken at this stage. The information obtained from exploration drilling wells is used to validate and revise the preliminary conceptual model of the geothermal reservoir. If at this stage the positive result is confirmed, the project sponsor will finalize detailed arrangements for project development. The activities at this stage are estimated to cost the project around US\$ 5 million.

5.1.3 Field development cost

The total cost associated with this stage is estimated to be US\$ 12.75 million. This cost includes the cost to drill a well-doublet system that consists of a production and an injection well. Other costs are allocated for the steam field facilities development. The geothermal drilling cost unit of a standard hole in Indonesia varies from US\$ 1,000/m up to US\$ 5,000/m depending on the location of the geothermal prospects [26]. A statistical analysis based on drilling data from 2011 to 2018 suggests USD 3,960/m is the mean value of the geothermal drilling cost unit in Indonesia [26]. Budisulistyo and Krumdieck [24] estimated the average drilling and development costs of a geothermal binary power plant in 2014 as \$1772 USD/kW.

5.1.4 Power plant construction cost

Power plant unit costs depend on power plant design (*i.e.* size and specification) and the components of power plant. DiPippo [15] describes that a basic binary power plant will be equipped by major equipment such as vaporizers and preheaters, condensers, organic vapor turbine, downhole pump, plant pumps and cooling tower.

Castle Rock Consulting [27] estimates the cost for equipment purchasing and power plant construction of a binary type of power plant as of US\$ 1.944/ kW gross. While Stefánsson [23] estimates the subsurface equipment can cost around 1000 USD/kW for a power plant capacity of 20–60 MW. In the case of Jaboi geothermal, we estimate the cost for power plant construction to be around US\$ 14.7 million.

5.1.5. Operational and maintenance cost

The total operational and maintenance costs for a 5 MW binary plant is estimated as US\$ 530.000 per year or US\$ 106 per kW. Assuming the power factor is 90 %, therefore the O&M cost is US\$ 2.8 cent/ kWh. Sanyal [28] estimates the operational and maintenance costs for a 5 MW typical geothermal power plant around US\$ 2.0 cent/kWh. Typically, the operational and maintenance cost for binary-type geothermal power plant is higher compared to a conventional (*i.e.*, flash system) geothermal power plant. The O&M cost for binary cycle geothermal power plant can be as high as US\$ 3.0 cent/kWh [29].

5.2 Economic Assessment Results

The economic feasibility of a power plant is evaluated by the internal rate of return (IRR). The selling price is simulated in the model at the range of USD 11 to 40 cent/kWh. As the comparison, the IRR is assessed based on pre-tax and after-tax profits with 30% of the tax rate.

The simulation shows the project is economically feasible when the selling price is over USD 30 cent/kWh which makes the IRR higher than 10% as shown in Figure 14. However, this selling tariff is significantly higher than the tariff agreed in Power Purchase Agreement (PPA) with the Indonesian National Electricity Company (PLN) which is USD 13.38

cent/kWh. Therefore, to be viable the option is either to increase the selling price or increase the generation capacity which is unlikely to be fulfilled in current situations. In the Indonesian electricity market, the selling tariff is regulated by the Ministry of Energy and Mineral Resources, therefore there will be a cap imposed. On the other hand, in the current state of electricity consumption, it is not possible to increase the generation capacity as to reach the electricity demand double as of now, it will take at least 15 years given the current electricity demand growth as shown in Figure 3.

Geothermal is the best source of renewable energy for Indonesia to reduce the emissions produced from energy sectors, however electricity produced from geothermal has to be competitive with the energy generated from fossil fuel sources [30]. Currently, the electricity in Weh Island is supplied from diesel generators. Therefore, to assess the economic competitiveness the geothermal binary cycle power plant, the authors compared the feasible price of electricity produced from Jaboi geothermal plant to the levelized cost of electricity (LCoE) produced from the diesel power plant for similar capacity. The levelized cost of electricity is a parameter that indicates constant electricity price required to achieve break-even point during the lifetime of the power plants [19]. To calculate the LCoE of electricity produced from the diesel power plant, we use data and assumptions as shown in Table 5.

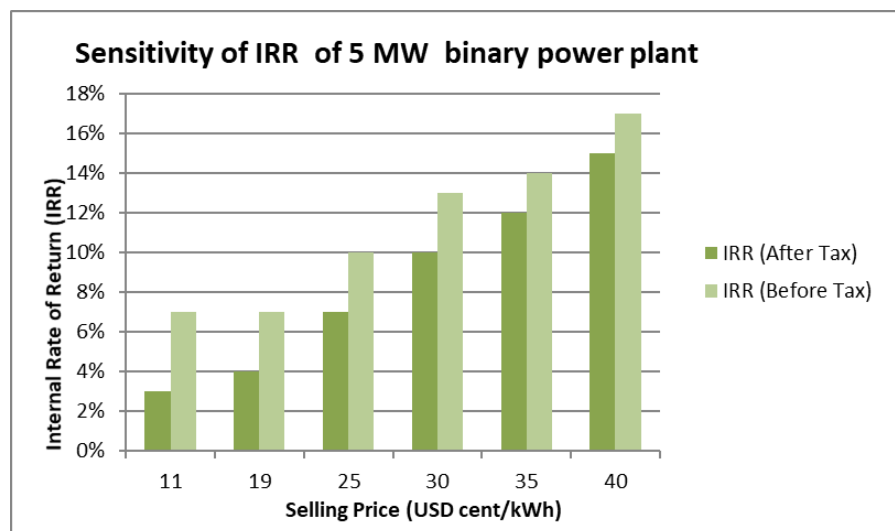


Fig. 14. Sensitivity of IRR to the electricity selling price.

Table 5. The parameters applied in calculating the levelized cost of electricity (LCoE) produced from a diesel power plant.

Parameter	Value
Diesel power plant capacity	5000 kW
Investment @ US\$ 500/kW	US\$ 2.500.000
Capacity factor	0.8
Annual electricity production	35 GWh
Fuel consumption	0.269 liter/kWh
Annual fuel cost @ US\$ 0.72/liter	US\$ 9.415.928
Annual O&M cost @ US\$ 0.198/kWh	US\$ 6.930.000

Source: Adapted from [31]

The levelized generation cost is calculated by using Equation 18:

$$LEC = \frac{\sum_{t=1}^n \frac{I_t + M_t}{(1+r)^t}}{\sum_{t=1}^n \frac{E_t}{(1+r)^t}} \quad (18)$$

where

LEC = levelized electricity cost in US\$/kWh

I_t = capital or investment cost in year t

M_t = operational and maintenance cost in year t

E_t = electricity generated in year t

r = the estimated discount rate (10%)

t = power plant lifetime

Based on LCOE calculation of a diesel power plant, to produce a kWh of electricity will cost US\$ 39 cent. This indicates that electricity produced from Jaboi geothermal by using binary cycle power technology is economically competitive.

6. CONCLUSION

The development of Jaboi geothermal resource in Weh Island has faced a long delay due to difficulties in finding its economic viability. This constraint surfaced because of Jaboi geothermal cannot be exploited to its full potential power estimation of 40 MW due to the electricity demand in the Island is very low. Therefore, a demand-based power plant shall be employed to optimize its economic values.

This paper proposes an alternative approach in utilizing small-scale geothermal resources that faces economic viability constraints. The authors propose a conceptual design of a geothermal binary cycle power plant adapted to the electricity demand available in the isolated grid such as in Weh Island, in this case with the application to Jaboi geothermal resources. In the aspect of resource capacity, Jaboi geothermal system can produce the brine with a temperature approximately 200°C which can be supplied from a geothermal well of 1000 m depth.

The power plant is designed to produce 3 MW net power output or approximately 5 MW in terms of gross power. The simulation results reveal that to produce 3 MW of net power output, the power plant requires 95 kg/s of brine flow rate that highly likely can be supplied from a production well. Within this scenario, therefore, a well-doublet system consisting of two wells of production and re-injection wells can be deployed. Furthermore, the simulation also indicates that as much as 32% of power production is used to power the auxiliary equipment.

Additionally, the authors attempt to analyze the economic viability and competitiveness of the Jaboi geothermal binary power plant if designed as a well-doublet geothermal system. It was found that to achieve IRR of at least 10%, the minimum selling price of USD 30 cent/kWh shall be fulfilled. Therefore, at current agreed selling price of USD 13.38 cent/kWh the geothermal project is not financially feasible. However, the LCoE analysis indicates that the Jaboi geothermal power plant is economically competitive compared to

currently electrical power produced from diesel power plants.

REFERENCES

- [1] Directorate General for New and Renewable Energy and Energy Conservation. *Statistik EBTKE 2015*, Retrieved February 17, 2022 from the World Wide Web: <http://ebtke.esdm.go.id/post/2016/02/02/1105/statistik.ebtke.2015>
- [2] Fauzi A., 2015. Geothermal resources and reserves in Indonesia: an updated revision. *Geotherm Energy Science*; 3, Retrieved February 17, 2022 from the World Wide Web: <http://www.geotherm-sci.net/3/1/2015/gtes-3-1-2015.pdf>.
- [3] Mahbaz S.B., Yaghoubi A., Dehghani-Sanij A., Sarvaramini E., Leonenko Y., and Dusseault M.B., 2021. Well-doublets: a first-order assessment of geothermal sedheat systems. *Applied Sciences* (11): 1–18.
- [4] Hochstein M.P. and P. Browne. 2000. Surface manifestations of geothermal systems with volcanic heat sources. In: Sigurdsson H (ed) *Encyclopedia of volcanoes*. Academic Press, p. 835.
- [5] Sumintadiredja P., Kasbani, Suhanto E., 2010. Jaboi. geothermal field boundary, Nangroe Aceh Darussalam, based on geology and geophysics exploration data. In: *World Geothermal Congress 2010*, Retrieved February 17, 2022 from the World Wide Web: <https://www.geothermal-energy.org/pdf/IGAstandard/WGC/2010/1169.pdf>
- [6] Dwipa S., Widodo S., Suhanto E., and Kusnadi D. 2006. Integrated geological, geochemical and geophysical survey in Jaboi geothermal field, Nangro Aceh Darussalam, Indonesia. In: *7th Asian Geothermal Symposium*. Qingdao: China, 25-26 July. Retrieved February 17, 2022 from the World Wide Web: https://www.geothermal-energy.org/pdf/IGAstandard/Asian/2006/20_dwipa.pdf.
- [7] Isa M., Cesarian D., and Abir I., 2020. Remote sensing satellite imagery and in-situ data for identifying geothermal potential sites: Jaboi, Indonesia. *The International Journal of Renewable Energy Development*, Retrieved February 17, 2022 from the World Wide Web: <https://doi.org/10.14710/ijred.9.2.237-245>
- [8] Muhammad R.A., 2009. *Eksplorasi energi panasbumi dengan dengan metode geofisika dan geokimia pada daerah Jaboi, Kota Sabang, Propinsi Nangroe Aceh Darussalam*. BSc Thesis, Institute Technology Bandung, Bandung, Indonesia.
- [9] Dirasutisna S. and A.R. Hasan. 2005. *Geologi Panas Bumi Jaboi, Sabang, Province Nangroe Aceh Darussalam*. Bandung: Report Direktorat Inventarisasi Sumber Daya Mineral.
- [10] Septian A.F., 2018. *Analisis Teknis dan Ekonomis Pemanfaatan Energi Panas Bumi di Area Jaboi*

- Sabang dalam Menunjang Sistem Kelistrikan di Sabang*. BSc Thesis, Universitas Sumatera Utara, Medan, Indonesia.
- [11] Pratama F., Reyseliani N., and Syauqi A.. 2020. Thermo-economic assessment and optimization of wells to flash–binary cycle using pure R601 and zeotropic mixtures in the Sibayak geothermal field. *Geothermics*, Retrieved February 17, 2022 from the World Wide Web: <https://doi.org/10.1016/j.geothermics.2019.101778>.
- [12] Heberle F. and D. Brüggemann. 2010. Exergy based fluid selection for a geothermal Organic Rankine Cycle for combined heat and power generation. *Applied Thermal Engineering* 30(11-12): 1326-1332
- [13] DiPippo R., 2008. *Geothermal power plants: principles, applications, case studies and environmental impact*. Oxford: Butterworth-Heinemann.
- [14] Franco A. and M. Villani. 2009. Optimal design of binary cycle power plants for water-dominated, medium-temperature geothermal fields. *Geothermics* 38(4): 379-391.
- [15] DiPippo R., 1999. Small geothermal power plant. Design, performance and economics. *GHC Bulletin*, Retrieved February 17, 2022 from the World Wide Web: <http://digitallib.oit.edu/digital/collection/geoheat/id/11217/>
- [16] Nur S., 2016. Utilization of Jaboi geothermal resources by using binary cycle power plant. In: *2016 Asian Alumni Workshop on Resilience in Energy System*, Retrieved February 17, 2022 from the World Wide Web: <https://www.uni-flensburg.de/fileadmin/content/abteilungen/developing-countries/dokumente/downloads/association-of-indonesian-alumni-of-university-of-flensburg-proceedings.pdf#page=52?cv=1>
- [17] Lukawski M., 2009. *Design and Optimization of Standardized Organic Rankine Cycle Power Plant for European Conditions*. Master's Thesis. University of Iceland, Reykjavik, Iceland
- [18] Frick S., Stefan K., and Saadat A., 2010. Holistic design approach for geothermal binary power plants with optimized net electricity provision. In: *World Geothermal Congress 2010*, Retrieved February 17, 2022 from the World Wide Web: https://gfzpublic.gfz-potsdam.de/pubman/faces/ViewItemOverviewPage.jsp?itemId=item_240738_1
- [19] Walraven D., Laenen B., and D'haeseleer W., 2015. Minimizing the levelized cost of electricity production from low-temperature geothermal heat sources with ORCs: Water or air cooled? *Applied Energy* 142: 144-153.
- [20] Arif M., 2006. *Pemboran landaian suhu sumur JBO-1 dan JBO-2 daerah panas bumi Jaboi, P. Weh, Kota Sabang-NAD (in Indonesian language)*. Pusat Sumber Daya Geologi.
- [21] Aksoy N., 2007. Optimization of downhole pump setting depths in liquid-dominated geothermal systems: A case study on the Balcova-Narlidere field, Turkey. *Geothermics* 36(5): 436-458.
- [22] Huenges E., 2010. *Geothermal energy systems. Exploration, development, and utilization*. Weinheim: Wiley-VCH.
- [23] Stefánsson V., 2001. Investment cost for geothermal power plants. *Geothermics* 31(2): 263-272.
- [24] Budisulistyo D. and S. Krumdieck. 2015. Thermodynamic and economic analysis for the pre-feasibility study of a binary geothermal power plant. *Energy Conversion Management* 103: 639-649
- [25] Purwanto E.H., 2019. *Assessment of Exploration Strategies, Results and Costs of Geothermal Fields in Indonesia*. (Report number: 22), United Nation University, Geothermal Training Programme, Iceland.
- [26] Purwanto E.H., 2018. Geothermal Drilling in Indonesia: a Review of Drilling Implementation, Evaluation of Well Cost and Well Capacity. In: *The 6th Indonesia International Geothermal Convention & Exhibition (IIGCE) 2018*, Retrieved February 17, 2022 from the World Wide Web: https://www.researchgate.net/publication/331649323_Geothermal_Drilling_in_Indonesia_a_Review_of_Drilling_Implementation_Evaluation_of_Well_Cost_and_Well_Capacity
- [27] Castlerock Consulting 2010. *Phase 1 Report: Review and Analysis of Prevailing Geothermal Policies, Regulations and Costs*, Jakarta, Indonesia.
- [28] Sanyal S.K., 2004. Cost of geothermal power and factors that affect it. In: *Twenty-Ninth Workshop on Geothermal Reservoir Engineering*. Stanford, Retrieved February 17, 2022 from the World Wide Web: <https://www.slb.com/resource-library/technical-paper/geothermal/sanyal-cost-of-geothermal-2004>
- [29] U.S. Department of Energy. Geothermal Electric Technology. 2016, Retrieved February 17, 2022 from the World Wide Web: <https://www.wbdg.org/resources/geothermal-electric-technology>
- [30] Nur S. and Seulawah. 2011. Agam Geothermal Power Plant development: the economic rationale and competitiveness with coal based power plant. *Aceh Sci J* 1: 5–6.
- [31] Yodha Yudhistira N, Agus D, Ibrahim B., 2011. Aplikasi pembangkit listrik tenaga panas bumi (PLTP)-Biner mengganti pembangkit diesel di daerah terpencil (in Indonesian Language). *PT PLN (Persero)*.
- [32] Nur S, Burton B., and Bergmann A., 2022. Evidence on optimal risk allocation models for Indonesian geothermal projects under PPP contracts. *SSRN Electron J*, Retrieved February 17, 2022 from the World Wide Web: <http://dx.doi.org/10.2139/ssrn.3991872>.